

Magic Angles in Fracture Surface Morphologies of Gelatin Hydrogels

T. Baumberger, C. Caroli, D. Martina, and O. Ronsin

INSP, UPMC Univ Paris 06, CNRS UMR 7588 140 rue de Lourmel, 75015 Paris France

(Dated: December 12, 2018)

The full 2D analysis of roughness profiles of fracture surfaces resulting from quasi-static crack propagation in gelatin gels reveals an original behavior characterized by (i) strong anisotropy with maximum roughness at V -independent symmetry-preserving angles (ii) For crack velocities V below a critical value, a cross-hatched regime due to straight macrosteps drifting at the same magic angles (iii) A marked increase with V of average roughness amplitude. This, together with previous results on other highly compliant, tough, polymeric networks, leads us to propose the existence of a new class of morphologies, controlled primarily by elastic non-linearities.

PACS numbers: 62.20.Mk, 83.80.Kn

Over the past two decades, considerable effort has been devoted to characterizing and understanding the statistical properties of the roughness of fracture surfaces in linear elastic disordered materials. Investigation of a wide variety of systems, ranging from brittle silica glass to ductile metallic alloys, has revealed the ubiquity of wide roughness spectra exhibiting self-affine characteristics on sizeable wavelength ranges. On the basis of analysis of height-height correlation functions in a single direction, E. Bouchaud *et al.* [1] first conjectured a fully universal behavior summed up into a single Hurst exponent. The discrepancies between the predictions of various subsequent theoretical models have pointed toward the importance of also investigating possible anisotropies of the scaling properties [2]. Work along this line indeed reveals different scaling exponents along the crack propagation direction and the (orthogonal) crack front one. From this, Ponson *et al.* [3] conclude that the self-affinity of the roughness is described by a Family-Vicsek scaling, hence by a set of two exponents. Within their new analysis, full universality is no longer the case since they evidence the existence of at least two classes of materials.

However, on the basis of their theoretical work, Bouchbinder *et al.* [4] have recently raised several new issues. In particular, they point to the necessity of a full 2D analysis of the correlations and find, when reexamining some experimental data, that a host of up to now unidentified exponents appear. They insist on the need to focus on the effects of departures from linear elasticity in the fracture process.

In this spirit we report here on the nature of surface morphologies resulting from the fracture of gelatin, a highly compliant thermally reversible hydrogel, in the strongly subsonic regime. We show that these surfaces present very striking anisotropic features. Namely, the rms roughness $R(\theta)$, measured along a direction at angle θ from the propagation one Ox , exhibits two symmetry-preserving maxima for $\theta = \pm\theta_m$. For gels with a fixed gelatin concentration, this “magic angle” θ_m is constant over more than one decade of both crack velocity V and solvent viscosity η . Moreover, below a critical, η -

dependent, velocity V_c a new dynamical regime develops, characterized by a cross-hatched (CH) morphology due to straight “macroscopic” steps of heights a few 100 μm , emerging from the above-described coexistent micrometric roughness. These steps are oriented at the same magic angles $\pm\theta_m$ as those revealed by the microroughness.

Very similar CH patterns have been observed previously on a covalently cross-linked hydrogel [5, 6] and on various elastomers, swollen or not [7]. This, together with our results, leads us to propose the existence of a new class of morphologies, characteristic of highly compliant random polymer networks in which fracture implies large crack tip opening displacements (CTOD) and strong elastic non-linearities at work in the near-tip region.

Experimental — Our fracture surfaces result from mode-I cracks propagating along the mid-plane of long, thin gelatin slabs (Fig. 1.a.), as described in detail in reference [8]. A displacement Δ of the rigid grips is imposed along Oy to the notched plate. After an initial transient, the crack reaches a steady regime at a velocity V which increases with the “energy release rate” \mathcal{G} imposed by the opening Δ . We found that, in this slow, subsonic regime ($V < 30$ mm/s), $\mathcal{G} = \mathcal{G}_0 + \Gamma\eta V$ with $\mathcal{G}_0 \simeq 2.5$ J.m⁻², $\Gamma \simeq 10^6$, and were able to assign this strong V -dependence to the fact that, in such a reversible gel, fracture occurs via scissionless chain pull-out, the high dissipation being due to viscous drag [8, 9].

tip Velocity (mm.s ⁻¹)	1.16	5.9	13.5	23.3
crack opening (mm)	5	7	9	11
rms roughness (μm)	2.5	3.1	4.1	5.3
angle θ_m (°)	18	17	17	22

TABLE I:

The results reported here were obtained on gels with a 5 wt.% content of gelatin in the solvent (pure water except when otherwise specified). The gel low-strain shear modulus $\mu = 3.5$ kPa (transverse sound speed ~ 1.9 m/s), is due to the entropic elasticity of the ran-

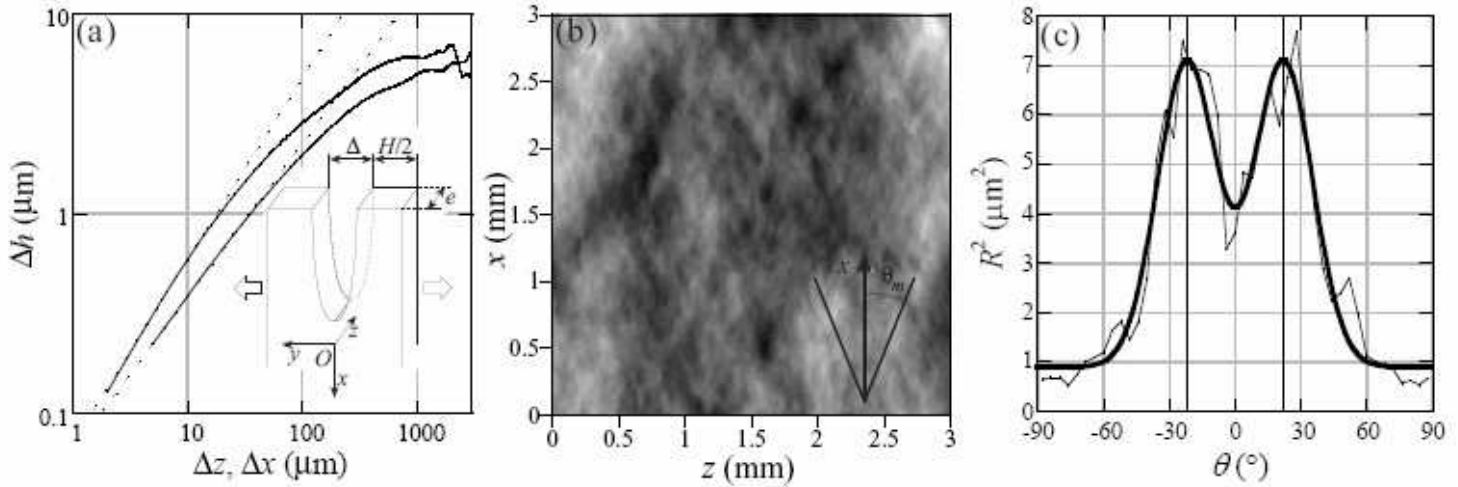


FIG. 1: Roughness characteristics for a 5 wt% gelatin/water gel for crack velocity $V = 13.5$ mm/s. (a) Plot of the height-height correlation functions $\Delta h_x(\Delta x)$ and $\Delta h_z(\Delta z)$ (see text). Insert : Schematic experimental geometry. Sample dimensions are : length $L = 300$ mm, height $H = 30$ mm, thickness $e = 10$ mm. (b) 3×3 mm² map of heights $h(x, z)$. The gray scale ranges over $27 \mu\text{m}$. The oblique lines correspond to peak positions in fig. 1.c. (c) Anisotropic squared roughness R^2 vs. angle θ measured from crack propagation direction. The dark line is the best fit with a sum of two Gaussians with an offset baseline.

dom polymer network, of average mesh size $\xi \sim 10$ nm. Note that, owing to this huge compliance, even very slow cracks ($V \sim 100 \mu\text{m/s}$) demand large openings Δ (Table I), typically $\gtrsim 3$ mm, comparable with the slab thickness e . Post-mortem replicas of crack surfaces, obtained by UV curing of a thin layer of glue, are scanned with the help of a mechanical profilometer (stylus tip radius $2 \mu\text{m}$, out of plane resolution 0.1 nm). Our maps $h(x, z)$ of heights above mean plane correspond to 3×3 mm² scans. Each one consists of a series of 600 lines parallel to the front direction Oz , each line containing 1500 data points.

The microrough morphology — For $V \gtrsim 300 \mu\text{m/s}$, the fracture surfaces are flat on the macroscale, yet clearly not mirror-like. As expected with such a material, elastic modulus as well as toughness fluctuations due to the randomness of the network result in in- and out-of-plane excursions of the crack front line, the profile roughness being the imprint of the latter ones. A typical map is shown in figure 1.b. For this crack velocity $V = 13.5$ mm/s, we find that the global rms roughness $\bar{R} = 4.1 \mu\text{m}$ [10]. Following Ponson *et al.* [3], we first characterize height correlations along the front (Oz) i.e. we compute : $\Delta h_z(\Delta z) = \langle [h(z + \Delta z, x) - h(z, x)]^2 \rangle_{z,x}^{1/2}$ and its counterpart $\Delta h_x(\Delta x)$ along the propagation direction (Ox). As indicated by figure 1.a. the microroughness spectrum is anisotropic and of the broad band type. However, at variance with the findings of [3], a simple power law fit (see dashed lines) is, here, clearly unconvincing. The discrepancy leads us, following Bouchbinder *et al.* [11], to try and exploit more extensively the full 2D

information. Indeed, naked-eye inspection under grazing incidence, as well as the aspect of height maps (Fig. 1.b.), strongly suggest the presence of preferred oblique directions. This suspicion we have confirmed by computing the angle-dependent squared roughness $R^2(\theta)$, obtained by integrating the power spectrum $|\hat{h}(\mathbf{q})|^2$ over an angular sector $d\theta = 4^\circ$ about angle $\theta + \pi/2$ (in \mathbf{q} -space) and in the wavelength window $2 \mu\text{m} - 1$ mm. We find in all cases that $R^2(\theta)$ exhibits two marked symmetric peaks at $\theta = \pm\theta_m$ (see figure 1.c. for which $\theta_m = 22^\circ$). Moreover (Table I), θ_m does not show any significant variation over the whole V -range ($V_{\max}/V_{\min} \sim 20$). In addition, a 10-fold increase of solvent viscosity η , obtained by using a 40/60 water/glycerol mixture, does not either affect its value.

Finally the full 2D-averaged rms roughness \bar{R} exhibits a clear quasi-linear V -dependence, a 20-fold V increase resulting in a 2-fold growth of \bar{R} (Table I).

The crosshatched (CH) morphology — When, starting from the microrough regime, we perform a step-by-step decrease of Δ , thus slowing down crack propagation. Below a critical velocity $V_c = 350 \pm 20 \mu\text{m/s}$ we observe on the fracture surfaces the emergence, at apparently random locations across the slab width, of oblique straight line defects (Fig. 2.a.). Upon further V decrease, these lines proliferate into a scale-like pattern, akin to the CH morphologies found by Tanaka *et al.* [5] on a covalently cross-linked gel and by Gent *et al.* [7] on elastomers. Moreover, optical imaging of the moving crack tip (Fig. 2.b.) permits to check that the associated drifting front defects have precisely the topology (Fig. 2.c.) identified

in [5] and [7]. The fold CC'DD' ultimately closes as the front proceeds, leaving two complementary steps on the crack faces.

Step nucleation profiles (see Fig. 2.d.) show that these macrodefects emerge via self-amplification of the micro-roughness, with which they coexist. Their height saturates, after a traveling distance of several millimeters, to values \sim a few $100\mu\text{m}$. No change of their drift angle is discernable as they grow, so that they propagate at the magic angle θ_m of the microroughness. We find it to remain V -independent over the full $V < V_c$ explored range.

Discussion — The above phenomenology presents several striking discrepancies with the known morphologies, pertaining to metallic alloys, silica glasses, quasicrystals, mortar, wood and sandstone [2]. Namely, none of these materials has been reported to exhibit (i) preferential anisotropy directions (ii) a CH regime (iii) a noticeable increase of \bar{R} with V in the quasistatic regime. On the other hand, these three a priori puzzling features are not restricted to gelatin gels. Indeed, as already mentioned, the CH regime has been documented for a chemical hydrogel and for elastomers. Moreover, using figure 5 of reference [6], one easily checks that, in their chemical gel as well, the CH drift angle is constant ($\theta_m \simeq 43^\circ$) over a 40-fold increase of V up to a critical V_c where the CH regime disappears.

The question then arises of which material features may be responsible for this new class of behavior. Two possible candidates are (a) poroelasticity, at work in hydrogels, and (b) the strong elastic non-linearities of these highly compliant solids.

(a) *Poroelasticity* — We have measured V_c for increasing viscosity η of the (water-glycerol) solvent. We find (Fig. 3) that $V_c = D_{\text{coll}}/d$ where the collective diffusion coefficient $D_{\text{coll}} \sim \mu\xi^2/\eta$, determined from dynamic light scattering, characterizes the solvent/network dissipative dynamics [12]. The constant length thus defined, $d \simeq 70\text{ nm}$, compares with the size ($\sim 100\text{ nm}$) of the process zone [9].

On the other hand we found that the magic CH angle in gelatin is η -independent. In the same line, Gent *et al.* [7] find θ_m to have the same value for an dry elastomer and for the same network swollen (ratio 2.6) with oil. This suggests that, while poroelasticity is irrelevant to the existence and value of magic angles, the dissipation associated with it could govern the nucleation of the “soliton-like” front defects responsible for macrostep generation.

(b) *Elastic non-linearities* — The behavior described above is obtained for slow, strongly subsonic cracks with large openings, since the very high compliance of gels and the large toughness of elastomers result in large remote strain levels even at the Griffith threshold. In this situation, the various theoretical models of self-affine roughness [2] are most probably inadequate, due to their com-

mon assumption of elastic linearity. We think that, here, non-linearities come into play through two effects. On the one hand a large Δ/H ratio certainly modifies the non-singular parts of the near-tip stress field (the so-called T- and A-stresses) known to control the response of the front to modulus and toughness fluctuations. On the other hand, in the tip region itself, the large non-linearities of the mechanical response laws, typical of polymer networks [13], certainly become crucial. Indeed, in the materials under consideration, critical decohesion stresses σ_c are much larger than low strain moduli (for our gelatin gels, $\sigma_c/\mu \sim 100$ [8]). This gives rise to elastic crack blunting [14] — a still open issue — as well as to strong anisotropy effects.

In our opinion a manifestation of the relevance of non-linearities lies in the behavior of the average roughness \bar{R} . Our cracks are quasi-static, so that front wave propagation [15] is irrelevant here, as confirmed by the constancy of θ_m . Hence the growth of \bar{R} with V should be understood as a dependence, not on propagation velocity proper, but on crack opening Δ , via the V -dependence of the fracture energy \mathcal{G} .

In conclusion we propose that the phenomenology brought to light and analyzed here is characteristic, beyond the case of gelatin gels, of a new class of morphologies of fracture surfaces, produced by quasi-static crack propagation in soft elastic materials tough enough to rupture at high strain levels. Putting this still somewhat conjectural statement on a completely firm basis will of course require further detailed investigations of the microroughness, e.g. on elastomers.

We are grateful to K. Sekimoto for stimulating interactions along the course of this work. We also thank M. Adda-Bedia, A. Argon, D. Bonamy, H. Brown, V. Lazarus for helpful discussions.

-
- [1] E. Bouchaud, J. Phys. Condens. Matter **9**, 4319 (1997).
 - [2] L. Ponson, *Crack propagation in disordered materials*, PhD Thesis, Ecole Polytechnique 2006 (unpublished) and references therein.
 - [3] L. Ponson, D. Bonamy, and E. Bouchaud, Phys. Rev. Lett. **96**, 035506 (2006).
 - [4] E. Bouchbinder, I. Procaccia, and S. Sela, J. Stat. Phys. **125**, 1029 (2006).
 - [5] Y. Tanaka, K. Fukao, Y. Miyamoto, and K. Sekimoto, Europhys. Lett. **43**, 664 (1998).
 - [6] Y. Tanaka, K. Fukao, and Y. Miyamoto, Eur. Phys. J. E **3**, 395 (2000).
 - [7] A.N. Gent and C.T.R. Pulford, J. Mat. Sci. **19**, 3612 (1984).
 - [8] T. Baumberger, C. Caroli, D. Martina, Nature Materials **5**, 552 (2006).
 - [9] T. Baumberger, C. Caroli, D. Martina, Eur. Phys. J. E

- 21**, 81 (2006).
- [10] Computation of the real surface area shows it to differ by less than 1% from the apparent (projected) one, so that the corresponding correction to the fracture energy is negligible.
 - [11] E. Bouchbinder, I. Procaccia, and S. Sela, Phys. Rev. Lett. **95**, 255503 (2005).
 - [12] T. Baumberger, C. Caroli, and O. Ronsin, Phys. Rev. Lett. **88**, 075509 (2002).
 - [13] A.N. Gent, Rubber Chem. Tech. **69**, 59 (1996).
 - [14] C.-Y. Hui, A. Jagota, S.J. Bennison, and J. D. Londono, Proc. Roy. Soc. Lond. A **459**, 1489 (2003).
 - [15] A. Livine, G. Cohen, and J. Fineberg, Phys. Rev. Lett. **94**, 224301 (2005).

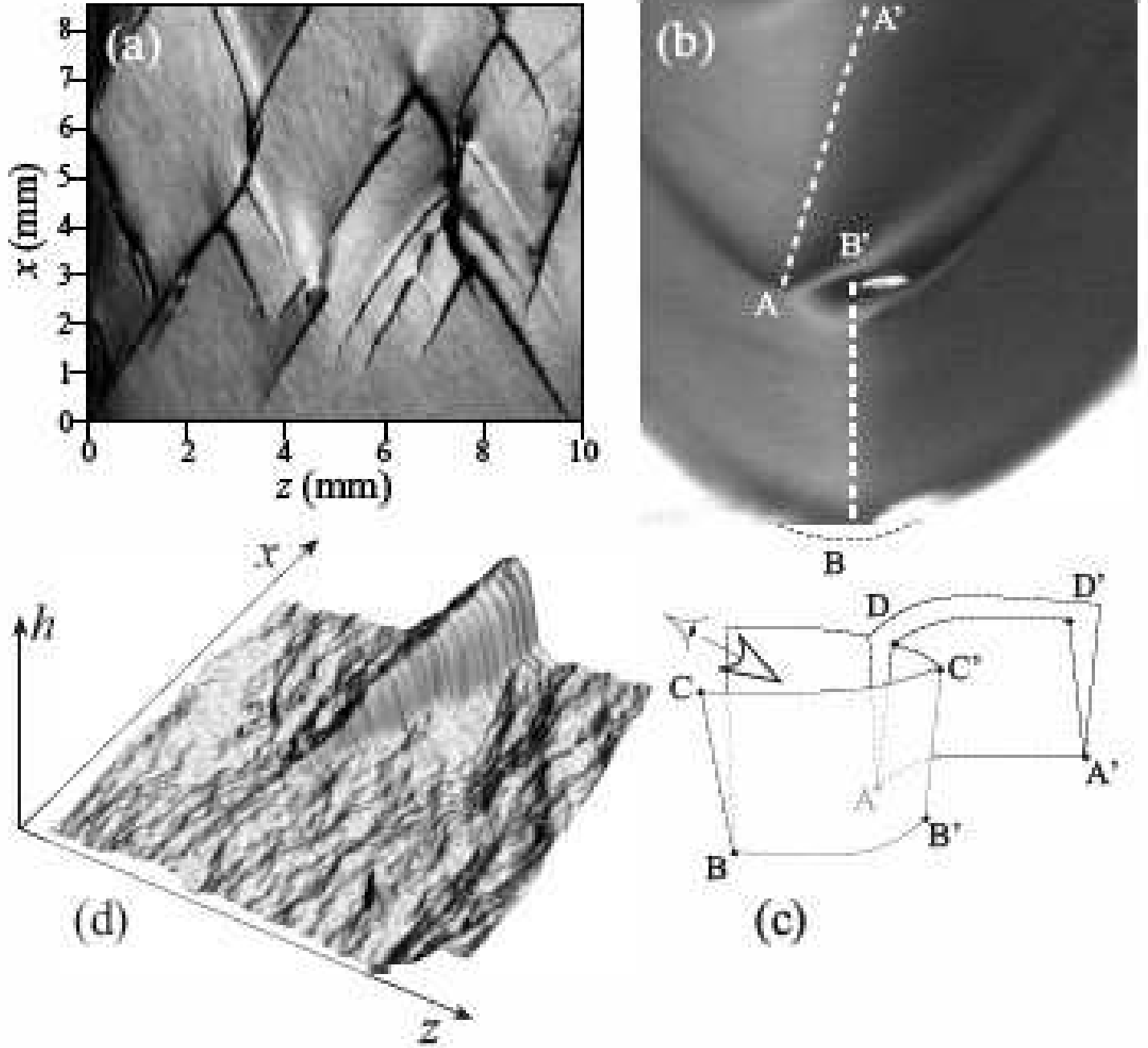


FIG. 2: Morphology in the cross-hatched regime. (a) optical imaging of a typical CH pattern. The crack propagates upward, its velocity being $V \lesssim V_c$ at bottom of image. (b) The moving crack tip region as imaged looking down in the Oxz plane at 45° from the Ox axis (insert of Fig. 1.a.). The white dashed line $A'B'$ indicates the frontline. The drifting front defect AB' leaves two complementary macrosteps on the crack faces. (c) Topological sketch of the front defect. The arrow indicates the direction of observation corresponding to figure 1.b. (adapted from ref.[5]). (d) 3D profile ($400 \times 400 \mu\text{m}^2$, $15 \mu\text{m}$ peak to peak) illustrating the emergence of a macrostep out of the microroughness ($V \lesssim V_c$).

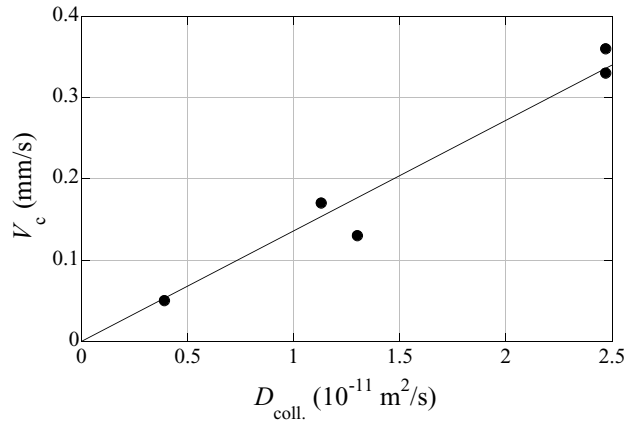


FIG. 3: Lower limit V_c of the microrough regime versus collective diffusion coefficient D_{coll} for 5 wt.% gelatin gels in solvents with various glycerol content. The line is a best linear fit.